RSC Advances

ROYAL SOCIETY OF CHEMISTRY

www.rsc.org/advances

Graphical Abstract

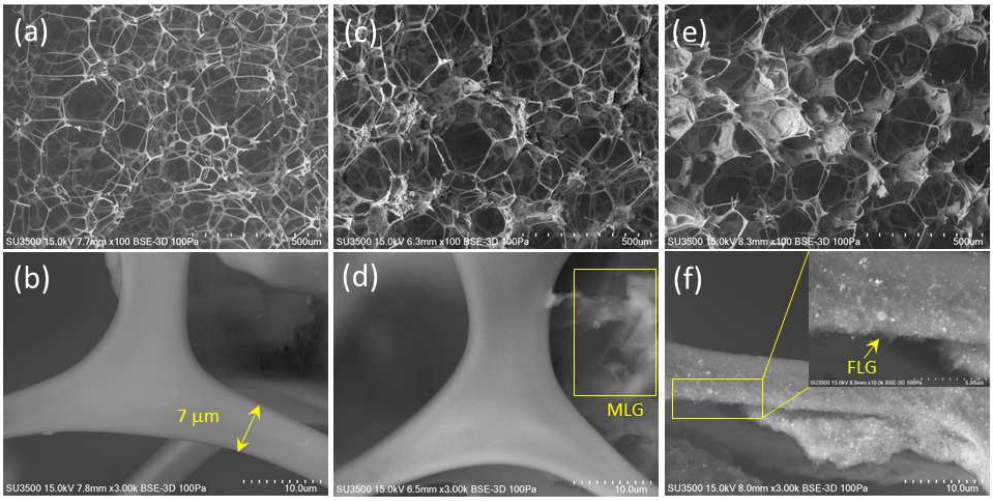

Few-layer Graphene based Sponge as a Highly Efficient, Recyclable and Selective Sorbents for Organic Solvents and Oils

Er-Chieh Cho,[a] Yu-Sheng Hsiao,*[b] Kuen-Chan Lee,*[c] and Jen-Hsien Huang,*[d]

Department of Clinical Pharmacy, School of Pharmacy, College of Pharmacy, Taipei Medical University, Taipei (Taiwan), 110, Department of Fragrance and Cosmetic Science, Kaohsiung Medical University, Kaohsiung (Taiwan), 80708, Department of Materials Engineering, Ming Chi University of Technology, New Taipei City (Taiwan), 24301, and Department of Green Material Technology, Green Technology Research Institute, Kaohsiung (Taiwan), 30010.

[b,]*Corresponding author. E-mail: yshsiao@mail.mcut.edu.tw. Telephone: +886-2-29089899 ext 4458. Fax: +886-2-29084091

[c,]*Corresponding author. E-mail: kclee@kmu.edu.tw. Telephone: +886-7-3121101 ext 2818. Fax: +886-7-3210683

[d,]*Corresponding author. E-mail:295604@cpc.com.tw. Telephone: +886-7-5824141 ext 7331. Fax: +886-7-5887302

[a]Department of Clinical Pharmacy, School of Pharmacy, College of Pharmacy, Taipei Medical University, Taipei (Taiwan).

[b]Department of Materials Engineering, Ming Chi University of Technology, New Taipei City (Taiwan).

[c]Department of Fragrance and Cosmetic Science, Kaohsiung Medical University, Kaohsiung (Taiwan).

[d]Department of Green Material Technology, Green Technology Research Institute, CPC Corporation, Kaohsiung (Taiwan).

In this work, we illustrate a facile and economical strategy for the bulk production of aqueous few layer graphene (FLG) dispersions via a simple grinding method. The as-prepared FLG suspensions can be cast on various substrates through facile dip coating. The environmentally friendly one-step procedure can produce graphene-based surface easily without additional reduction reaction. Here, we also prepare the FLG-based sponges with both superhydrophobic and superoleophilic properties. The FLG-sponges have been demonstrated as efficient absorbents for a broad range of oils and organic chemicals with high selectivity and excellent recyclability. The FLG-sponges deliver an absorption capacity as high as 153 g g-1 for the chloroform. The results indicate that the FLG sponges may potentially be useful as next-generation oil adsorbent materials.

1. Introduction

Recently, the world is facing a serious environmental crisis due to the waste of water resource and industrial pollutions such as oil spill and chemical leakage. With the awareness of environmental protection, the technological developments for water recycling, removal of oil spill and organic contaminants have become increasingly important. Oil sorbent materials such as porous polymers,[1] inorganic based materials[2-5], carbon nanotube or other carbon-based composites[6-17] and other composites[18-21] have been developed to meet the demand of water purification and cleanup of oil pollution. These proposed materials, however, have some drawback including low absorption capacity, poor selectivity and environmental incompatibility. Moreover, these materials are expansive and prepared from complicated process leading to the limitation of practical application

To address this issue, the graphene-based materials have been proposed. The oil absorbent based on commercial sponges coated with graphene oxide (GO) have been successfully prepared through dip coating method.[22-27] Although the GO is hydrophilic, its hydrophobic property still can be recovered via reduction process to form reduced graphene oxide (rGO).[28] The rGO based absorbents reveal high absorbency, selectivity and recyclability. Unfortunately, in most cases, the reduction process cannot completely transform the GO into rGO. Therefore, trace amount of hydrophilic oxygen-containing

groups still remain in rGO. This not only limits the hydrophobic property of the resulting rGO, but also influences its selectivity, significantly. Moreover the complicated reduction processes are unfavorable for industrial application. The drawback of GO-derived absorbent has been overcome by growing three dimensional (3D) graphene using chemical vapor deposition (CVD).[29] The defect-free 3D graphene can selectively remove oils and organic solvents from water owing to its superhydrophobic and superoleophilic properties. However, the CVD-grown approach is time and energy-consuming and difficult to scale up for practical use.

Recently, the multilayer graphene (MLG, 50-100 nm) has been commercial available. These products are prepared through scalable, facile and economical approaches such as electrochemical,[30,31] liquid-phase[32,33] or mechanical exfoliation.[34] The commercial MLG without structural and chemical defects reveals excellent optoelectronic and thermal properties. However, the large bulk density of MLG makes it easily precipitate out in a solution. Therefore, it also suffers from poor processability and mechanical property due to its unfuctionalized, graphite-like structure. In this study, we used a wet grinding method to disperse the MLG. During the surfactant-assisted grinding process, MLG underwent further exfoliation and miniaturization in submicron scale to form a stable dispersed solution containing FLG. The ground FLG with great processability can be easily cast on various substrates through solution process. We also fabricate the MLG-based absorbent using commercial melamine sponge as frame. The as-prepared absorbent exhibits excellent superhydrophobic and superoleophilic proterties with high absorption capacity and recyclability for a wide range of organic compounds. It is believed that the FLG-based absorbent will have great potential for large-scale oil-water separation.

2. Experimental Section

2.1 Preparation of FLG dispersions:

MLG (P-ML20) was purchased from Enerage Inc. The thickness of MLG are ranged between

50~100 nm. High-energy ball milling was performed at room temperature using a batch-type grinder (JBM-B035).[35] The total milling duration was 360 min; the concentration of MLG was 5.0 wt%. The grinding procedure was performed in isopropyl alcohol containing 0.1 wt% sodium dodecyl sulfate (SDS). The MLG solution was ground under 2000 rpm with ZrO_2 (200 nm) as milling ball for 3 hr. Consequently, the resultant MLG solution was further ground with smaller ZrO_2 (100 nm) to enhance the dispersability of FLG. After high-energy grinding, the FLG suspensions can be diluted to any concentration without precipitation.

2.2 Preparation of FLG-based absorbents

The commercial melamine sponge was cut into blocks (2 x 2 cm^2) and ultrasonically cleaned in ethanol. Then, the blocks were rinsed with distilled water and dried at 70 ^oC. The as-dried sponge was then dipped into the ground FLG solution, and finally dried in the vaccum oven at 100 ^oC. The FLG can be physically coated on the sponge due to the strong van der Waals interaction and mechanical flexibility of FLG. Finally, the treated sponge was immersed into a dilute toluene solution which contains PDMS followed by drying at 120 ^oC overnight to enhance the adhesion between the FLG and the sponge.

2.3 Characterization

Zeta potentials were measured using a particle size analyzer (Brookhaven 90 Plus Sn11408). XRD was performed using a Philips X'Pert/MPD apparatus. The surface morphologies of the FLG films were investigated using AFM (Digital Instrument NS 3a controller equipped with a D3100 stage) and SEM (Hitachi S-4700). The absorption capacities (k) of FLG-based sponges for various organic solvents were measured. A weighed amount of FLG sponge was put into a flask containing of organic solvent and allows to absorb for 5 min. Then k can be calculated through the definition, $k=(W_{saturated\ absorption}-W_{initial})/W_{initial}$.

3. Results and Discussion

The SEM images of the commercial MLG are shown in Fig. 1. It can be observed that the commercial products contain a large amount of graphene flasks with a curled morphology consisting of a wrinkled paper-like structure. The images reveal that the MLGs have a size of several tens of microns and they are stack from several graphene sheets (around 50-100 nm). Due to its large size and thickness, the MLG is difficulty to be dispersed in common organic solvents and cast on various substrates. With this regard, in this study, we performed the wet grinding method to treat the MLG. During the grinding process, the MLG experiences further exfoliation to form the FLG. Moreover, the size can also be reduced which can enhance its dispersability.

The TEM images of the MLG before and after grinding are shown in Fig.2. Compared with the ground sample (FLG), the MLG reveal a much dark TEM image. This is due to its stacked multilayer leading to the electron non-transparency. In contrast, the FLG reveals a very transparent image indicating that the thickness of MLG has been successfully reduced after grinding process. Moreover, after grinding procedure, the size of MLG also significantly decreases from several tens of micros to 200~500 nm. The crystallinity of the MLG, FLG and graphite was also measured by XRD analysis. As shown in Fig. 2c, it can be seen all the samples exhibit a characteristic peak (002) at 26.8^{o}. However, the FLG show a much weak intensity compared with that of MLG and graphite. The full widths at half maximum (FWHM) of MLG and FLG obtained from XRD spectra is shown in the Supporting Information. Compared with MLG, the larger FWHM of FLG is contributed from the further exfoliation and miniaturization during the grinding treatment. In general, the FLG should be more highly charged and, therefore, possess enhanced dispersibility compared with the MLG owe to its higher degree of exfoliation and smaller size.[36] To investigate the correlation between the surface charge of the FLG and the grinding time, we measured the zeta potential of the FLG solution with different grinding time. As shown in Fig. 2d, there is a trend towards more negative zeta potential values as the grinding time is increased. This suggests that the grinding process miniaturizes and exfoliates the MLG leading to higher edge-to-area ratio, which increases their charge density and repulsive electrostatic force. Moreover, the surfactant (SDS) also can wrap the FLG which changes the FLG's surface chemistry leading to more

negative zeta potential and better dispersion. This phenomenon is similar to the zeta-potential variation of surfactant-wrapped carbon nanotubes.[37,38] The inset to Fig. 2d provides images of the FLG solutions after various grinding times. It can be found that the FLG can disperse very well. However, the MLG without grinding treatment tends to precipitate easily. The FLG colloids can maintain its stability without precipitation over 3 months. It is well known that the colloidal stability of graphene is determined by the competition between repulsive electrostatic interaction and attraction, face-to-face van der Waals interaction of overlapping sheets.[39,40] We believe that the better colloidal stability of FLG after grinding is contributed from the combination of increased electrostatic repulsion and reduced overlapping area due to the further exfoliation and miniaturization.

Absorption spectroscopy can be used to further shed light on the dispersability of the FLG colloidals. The absorption spectra are acquired by a UV-vis spectrometer with a wavelength of 200-800 nm at different concentrations of FLG from 0.01 to 0.25 wt% as shown in Fig. 3a. All the spectra reveal an absorption peak located at 265 nm which is originated from the electronic π–π^* transition of C=C bounds.[41] A linear relationship can be seen in the inset of Fig. 3a and follows the Lambert-Beer law well,[42] suggesting that the FLG can form an uniform and stable colloidal after grinding. Fig. 3b shows the Raman spectrum of the as-prepared FLG. The characteristic peaks located at 1340, 1577 and 2695 cm^{-1} corresponding to the D, G and 2D bands are observed. These characteristic peaks are associated with the disorder sp^3-hybridized carbon, E_{2g} vibrational mode of sp^2-bonded carbon and second-order vibration caused by the scattering of phonons, respectively.[43, 44] The inset of Fig. 3b reveals the XPS spectrum of FLG. It is seen that the C1s spectrum of FLG exhibits a sharp peak characteristic of single-phase pristine graphene flakes, suggesting the absence of oxygen-contained group within FLG. The XPS and Raman spectra for graphite and MLG are also shown in the Supporting Information. To monitor the thickness and size of the FLG, we also utilized the AFM to analyze the FLG cast on a silicon wafer. The typical AFM image of FLG is shown in Fig. 3c. The AFM and its corresponding surface profile for MLG is also shown in the Supporting Information. The uniformly distributed individual FLG sheets

with grain size ranged from 50 to 700 nm indicating the FLG is well-dispersed in the solution. Moreover, the thickness of FLG distributed from 3 to 11.5 nm with an average thickness of 7.7 nm is obtained through taking 100 FLGs into calculation as shown in Fig. 3d and 3e. The AFM observations further reveal that the MLG indeed experiences exfoliation and miniaturization during the grinding process

The porous structure of the melamine sponge, MLG-sponge and FLG-sponge was observed by SEM and is shown in Fig. 4. It can be seen that the sponge reveals three-dimensional, fiber-like structure with pore size ranged from 70-250 μm. The surface of hierarchical structure is very smooth and the diameter is found to be 7 μm. The images of MLG-sponge are shown in Fig. 4c and 4d. It can be clearly seen that the MLG cannot deposited on the surface of the fiber-like structure due to its too large size (several tens of micros, Fig. 1). The MLG only can stack in the pore formed by the three-dimensional structure after dip coating. In contrast, the FLG can be successfully deposited on the surface of the fiber-like surface (Fig. 4e and 4f). The FLG can be physically coated onto the sponge surface because of its mechanical flexibility and the van der Waals force between the sponge and FLG. The fiber-like structure shows a much rough surface with great surface coverage after FLG coating. This is contributed from the miniaturization and exfoliation during the grinding process. The small size and thickness of FLG can enhance its flexibility. As a result, the FLG can fold easily on various substrates with different shape.

To determine the hydrophobicity of the modified-sponge, the contact angle was measured. The relationship between coating times and water contact angle has been investigated, as shown in Fig. 5. As the coating time increases, the contact angle can also increase from 92.6^{o} (one time) to 143.5^{o} (three times) and the water droplet maintain a spherical shape as shown in Fig. 5. In contrast, a drop of water completely spread out and was infused into the bare sponge as shown in Fig. 5e (the water was dyed with methylene blue). Moreover, the FLG-sponge can immediately absorb lubricating oil and no contact angle can be measured. These results indicates that the FLG-sponge is superhydrophobic and oleophilic. The strong hydrophobicity is attributed from the combination of natural hydrophobic characteristic of

graphene and the surface roughness caused by the dual effect of wrinkled and folded FLG and hierarchical structure of the sponge. For the coating time larger than three times, the contact angle is unchanged, suggesting the surface of sponge has been covered by FLG completely. It is worthy to mention that the MLG-sponge cannot reveal the superhydrophobic and oleophilic property even though the coating times has been over ten. Furthermore, the color of the MLG-sponge is much lighter than that of FLG-sponge, as shown in Fig. 5f. This indicates that the MLG cannot be efficiently deposited on the sponge surface owe to its large volume and thick morphology.

The TGA analysis was performed to monitor the amount of the carbon-based materials deposited on the sponge surface. The weight loss for FLG occurred before 300 ^{o}C probably results from the evaporation of moisture and decomposition of SDS. As shown in Fig. 6, for the TGA curves of pure and modified sponges are similar and have a rapid weight loss for the temperature higher than 400 ^{o}C. This suggests the deposited amount of graphene is too small to influence the decomposition behavior. However, a slight difference for the total weight loss still can be observed. The residual weights of the sponge, MLG-sponge and FLG-sponge are 1.83, 6.05 and 10.08 wt%, respectively. These results further support the FLG can be more easily deposited on the sponge surface due to its favorable morphology.

For the practical application in oil-spill cleanups, the flotation of sponge on the top of water surface is crucial. As shown in Fig. 7a, the FLG-sponge can float on the surface of water. Even though we immerse the FLG-sponge in water with external force, the FLG-sponge can immediately float on the water surface after releasing the external force. Moreover, the mirror-like reflection can be found in the immersed part of FLG-sponge (Fig. 7b), due to the formation of an entrapped air between the FLG-sponge and the surrounding water. This phenomenon is referred to the so-called non-wetting Cassie–Baxter surfaces.[45,46] However, the untreated sponge submerged in the water within 3s (also see Movie S1). To demonstrate the separation ability, we put the FLG-sponge in a stable water/oil emulsions as depicted in Fig. 7c. To our surprise, the emulsified oil/water mixtures were well-separated and efficiently collected within the FLG-sponge after shaking the mixture for 5s (also see Movie S2). The water/oil emulsion before and after separating with FLG-sponge was further analyzed by an optical

microscope (Fig. 7d and 7e). It can be seen that all the oil microemulsions are absorbed by the FLG-sponge, indicating this technology can be used to collect the expansive chemical for the water/oil emulsions. As exhibited in Fig. 7f, the removal of the oil on the water surface was also tested. When the FLG-sponge is brought into contact with a layer of motor oil (CPC Corp.), it absorbs the oil completely within 3s (also see Movie S3). This clearly indicates its potential use for the facile removal of oil spillage and chemical leakage. Various organic solvents were used to further evaluate the absorption capacity and selectivity of the FLG-sponge. As shown in Fig. 7g, the absorption capacities of the FLG-sponge for a wide variety of organic solvents range from 57 to 153 times their weight. The variation of the capacity is caused by the density of oils and organic compounds. Compared with the nanowire membranes (<20 times)[2] and micro-porous polymer (<33 times),[1] the FLG-sponge can deliver much higher absorbance capacity. The recyclability of the FLG-sponge was also tested to evaluate its oil/chemical cleanup application. Fig.7h shows the recyclable use of the FLG-sponge for removal of chloroform, ethanol and pump oil. It can be seen that no obvious change was found after 20 cycles, indicating the excellent recycling performance.

4. Conclusion

In summary, we have developed a novel approach to prepare the stable, well-dispersed FLG colloidal. This facile, inexpensive and efficient method is easy to scale up for practical use. By dip coating with sponge, the FLG-sponges reveal superhydrophobic and superoleophilic properties. The FLG-sponges are ready to use for oil adsorption with high capacity and selectivity and oil loading have been demonstrated without producing any additional pollution. The FLG-sponges can be recycled and repeatably use via a simple method of distillation or squeezing. We believe that the modified-sponge is a promising candidate for large-scale removal of oil or organic solvent spills, recovery of chemicals and barrier separation.

ACKNOWLEDGMENT

We are grateful to the Ministry of Science and Technology (MOST 103-2218-E-037-001), Kaohsiung Medical University (KMU) (KMU-Q103001) and CPC Corp. for financial support. We would also like to thank the research fundings from Taipei Medical University, and Ministry of Science and Technology (TMU102-AE1-B02, TMUTOP103004-2, MOST103-2320-B-038-006-MY2). The research endeavors at Ming Chi University of Technology were supported by the Ministry of Science and Technology (MOST) of Taiwan (contract MOST 103-2221-E-131-002-MY2).

FIGURE CAPTIONS

Figure 1. The SEM images of the MLG. The MLG reveals a size of several tens of microns and stacked from several graphene sheets.

Figure 2. FLG prepared from grinding process. (a) TEM image of the MLG sample without grinding treatment; (b) TEM image of the FLG with grinding for 300 min; (c) XRD patterns of the graphite, MLG and FLG; (d) Zeta-potential measurment of FLG with differnet grinding times. (Inset: Images of the FLG solutions after various grinding times). The MLG can experience further exfoliation during brinding treatment, resulting in stable colloidal dispersion over 3 months without precipitation.

Figure 3. Characterization of the as-prepared FLG. (a) UV-vis spectra of FLG dispersion at different concentrations. Inset is a plot of absorption intensity versus FLG concentration; (b) Raman spectra of MLG and FLG. Inset is XPS spectrum of FLG; (c) a typical AFM image of FLGs on SiO_2 substrate. Scale bar: 5 □m; (d) AFM image of a single FLG with smooth planar structure. Scale bar: 250 nm; (e) thickness distribution of 100 FLG sheets. The thickness and sheet size of MLG can be reduced significantly during the grinding process leading to well-dispersed FLG solution.

Figure 4. The typical SEM images of the pure and modified sponges with different magnification. (a, b) pure sponge; (c, d) MLG-sponge and (e, f) FLG-sponge. Inset is the higher magnification SEM image. It can be seen that the FLG reveal a better mechanical flexibility due to its favorable morphology.

Therefore, it can be easily deposited on the surface of the sponge through the strong van der Waals interactions between the sponge and FLG.

Figure 5. Superhydrophobic property of FLG-sponge. Optical image of water droplet on FLG-sponge with different coating time. (a) one time; (b) two times; (c) three times; (d) relationship between coating time and contact angle of the FLG-sponge; (e) photograph of a water droplet on the surface of (e) FLG-sponge (black color) and pure sponge (white color); (f) MLG-sponge (gray color) and FLG-sponge. The water has been dyed with methylene blue. It can be seen that the water droplet can be supported and maintain a quasi-sphere shape on the surface of FLG-sponge, indicating its superhydrophobic property. However, the water droplets were immediately absorbed by the pure sponge and MLG-sponge.

Figure 6. The TGA curves of bare sponge, FLG-sponge, MLG-sponge and FLG powder. The residual weight of FLG-sponge is larger than that of MLG-sponge after heating at 900 ^{o}C, suggesting that the physically adhesive amount of graphene is larger. This is contributed form the better mechanical flexibility and smaller size of FLG compared with that of MLG.

Figure 7. The oil asorption performance of FLG-sponge. (a) photograph of bare sponge and FLG-sponge after being placed on water; (b) mirror-reflection can be observed when the FLG-spongewas immersed into water, which is a convictive and direct evidence for proving the hydrophobicity of FLG-sponge; (c) photographs of the water/toluene emulsion before and after separation; (d) the optical microscope images of the water/toluene emulsion before and (e) after separation; (f) snapshots of the removal process of motor oil by using FLG-sponge; (g) absorption capacity of the FLG-sponge on various organic liquids and oils. k here is defined as $k=(W_{saturated\ absorption}-W_{initial})/W_{initial}$. (h) absorption recyclability of the FLG-sponge for chloroform, ethanol and pump oil.

REFERENCES

(1) A. Li, H. X. Sun, D. Z. Tan, W. J. Fan, S. H. Wen, X. J. Qing, G. X. Li, S. Y. Li and W. Q. Deng, *Energy Environ. Sci*., 2011, **4**, 2062.

(2) J. Yuan, X. Liu, O. Akbulut, J. Hu, S. L. Suib, J. Kong and F. Stellacci, *Nat. Nanotechnol*., 2008, **3**, 332.

(3) Z. C. Ma, L. M. Wang, D. Q. Chu, H. M. Sun and A. X. Wang, *RSC Adv*. 2015, **5**, 27398.

(4) R. Arora and K. Balasubramanian, *RSC Adv*. 2014, **4**, 53761.

(5) W. Liang, Y. Liu, H. Sun, Z. Zhu, X. Zhao, A. Li and W. Deng, *RSC Adv*. 2014, **4**, 12590.

(6) X. C. Gui, J. Q. Wei, K. L. Wang, A. Y. Cao, H. W. Zhu, Y. Jia, Q. K. Shu and D. H. Wu, *Adv. Mater*., 2010, **22**, 617.

(7) H. Wang, Y. Gong and Y. Wang, *RSC Adv*., 2014, **4**, 45753.

(8) C. F. Wang and S. J. Lin, *ACS Appl. Mater. Interfaces*., 2013, **5**, 8861.

(9) M. N. Kavalenka, A. Hopf, M. Schneider, M. Worgull and H. Hölscher, *RSC Adv*., 2014, **4**, 31079.

(10) Y. Gao, Y. S. Zhou, W. Xiong, M. Wang, L. Fan, H. Rabiee-Golgir, L. Jiang, W. Hou, X. Huang, L. Jiang, J. F. Silvain, and Y. F. Lu, *ACS Appl. Mater. Interfaces* 2014, **6**, 5924.

(11) H. Bi, X. Huang, X. Wu, X. Cao, C. Tan, Z. Yin, X. Lu, L. Sun and H. Zhang, *Small* 2014, **10**, 3544.

(12) Y. Yang, Q. Zhang, S. Zhang and S. Li, *RSC Adv*., 2014, **4**, 5568.

(13) L. Peng, H. Li, Y. Zhang, J. Su, P. Yu and Y. Luo, *RSC Adv*., 2014, **4**, 46470.

(14) X. Gui, Z. Zeng, Z. Lin, Q. Gan, R. Xiang, Y. Zhu, A. Cao and Z. Tang, *ACS Appl. Mater. Interfaces* 2013, **5**, 5845.

(15) J. N. Wang, Y. L. Zhang, Y. Liu, W. Zheng, L. P. Lee and H. B. Sun, *Nanoscale* 2015, **7**, 7101.

(16) Y. L. Zhang, H. Xia, E. Kim and H. B. Sun, *Soft Matter* 2012, **8**, 11217.

(17) H. P. Cong, X. C. Ren, P. Wang and S. H. Yu, *ACS Appl. Mater. Interfaces* 2012, 6, 2693.

(18) F. Zhao, L. Liu, F. Ma and L. Liu, *RSC Adv.* 2014, **4**, 7132.

(19) L. Zhang, J. Wu, X. Zhang, G. Gong, J. Liu and L. Guo, *RSC Adv*. 2015, **5**, 12592.

(20) C. Chen, R. Li, L. Xu and D. Yan, *RSC Adv*. 2014, **4**, 17393.

(21) P. Xi, L. Huang, Z. Xu, F. Chen, L. An, B. Wang and Z. N. Chen, *-1*

2014, **4**, 59481.

(22) D. D. Nguyen, N. H. Tai, S. B. Lee and W. S. Kuo, *Energy Environ. Sci*., 2012, **5**, 7908.

(23) G. Wei, Y. E. Miao, C. Zhang, Z. Yang, Z. Liu, W. W. Tjiu and T. Liu, *ACS Appl. Mater. Interfaces*., 2013, **5**, 7584.

(24) Y. Liu, J. Ma, T. Wu, X. Wang, G. Huang, Y. Liu, H. Qiu, Y. Li, W. Wang and J. Gao, *ACS Appl. Mater. Interfaces*., 2013, **5**, 10018.

(25) H. Sun, Z. Zhu, W. Liang, B. Yang, X. Qin, X. Zhao, C. Pei, P. La and An Li, *RSC Adv*., 2014, **4**, 30587

(26) S. J. Yang, J. H. Kang, H. Jung, T. Kim and C. R. Park, *J. Mater. Chem. A*, 2013, **1**, 9427.

(27) B. Ge, Z. Zhang, X. Zhu, X. Men, X. Zhou, Q. Xue, *Compos. Sci. Technol*., 2014, **102**, 100.

(28) S. Pei, H. M. Cheng, *Carbon* 2012, **50**, 3210.

(29) X. Dong, J. Chen, Y. Ma, J. Wang, M. B. Chan-Park, X. Liu, L. Wang, W. Huang and P. Chen, *Chem. Commun*., 2012, **48**, 10660

(30) J. Wang, K. K. Manga, Q. Bao and K. P. Loh, *J. Am. Chem. Soc*., 2011, **133**, 8888.

(31) C. Su, A. Lu, Y. Xu, F. Chen, A. N. Khlobystov and L. Li, *ACS Nano*, 2011, **5**, 2332.

(32) N. Behabtu, J. R. Lomeda, M. J. Green, A. L. Higginbotham, A. Sinitskii, D. V. Kosynkin, D. Tsentalovich, A. N. G. Parra-Vasquez, J. Schmidt, E. Kesselman, Y. Cohen, Y. Talmon, J. M. Tour and M. Pasquali, *Nat. Nanotechnol*., 2010, **5**, 406.

(33) W. Lu, S. Liu, X. Qin, L. Wang, J. Tian, Y. Luo, A. M. Asiri, A. O. Al-Youbicd and X. Sun, *J. Mater. Chem*., 2012, **22**, 8775.

(34) M. Mao, S. Chen, P. He, H. Zhang and H. Liu, *J. Mater. Chem. A*, 2014, **2**, 4132.

(35) J. H. Huang, C. P. Li, C. W. C. Jian, K. C. Lee and J. H. Huang, *J. Taiwan Inst. Chem. E.* 2015, **46**, 168.

(36) J. Luo, L. J. Cote, V. C. Tung, A. T. L. Tan, P. E. Goins, J. Wu and J. Huang, *J. Am. Chem. Soc*., 2010, **132**, 1766.

(37) S. Pei, J. Du, Y. Zeng, C. Liu and H. M. Cheng, *Nanotechnology* 2009, **20**, 235707.

(38) J. S. Moon, J. H. Park, T. Y. Lee, Y. W. Kim, J. B. Yoo, C. Y. Park, J. M. Kim and K. W. Jin, *Diam. Relat. Mater.* 2005, **14**, 1882.

(39) L. J. Cote, F. Kim, J. Huang, *J. Am. Chem. Soc*., 2009, **131**, 1043.

(40) J. N. Israelachvili, *Intermolecular and Surface Forces*, 2nd ed. Academic Press: San Diego, 1992.

(41) D. D. Nguyen, N. H. Tai, Y. L. Chueh, S. Y. Chen, Y. J. Chen, W. S. Kuo, T. W. Chou, C. S. Hsu and L. J. Chen, *Nanotechnology*, 2011, **22**, 295606.

(42) J. D. J. Ingle and S. R. Crouch, *Spectrochemical Analysis*, Englewood Cliffd, NJ: Prentice Hall, 1988, p 372.

(43) A. C. Ferrari, J. C. Meyer, V. Scardaci, C. Casiraghi, M. Lazzeri, F. Mauri, S. Piscanes, D. Jiang, K. S. Novoselov, S. Roth and A. K. Geim, *Phys. Rev. Lett*., 2006, **97**, 187401.

(44) L. M. Malard, M. A. Pimenta, G. Dresselhaus, M. S. Dresselhaus, *Phys. Rep*., 2009, **473**, 51.

(45) A. B. D. Cassie, S. Baxter, *Trans. Faraday Soc*., 1944, **40**, 546.

(46) I. A. Larmour, S. E. J. Bell and G. C. Saunders, *Angew. Chem., Int. Ed*., 2007, **46**, 1710.

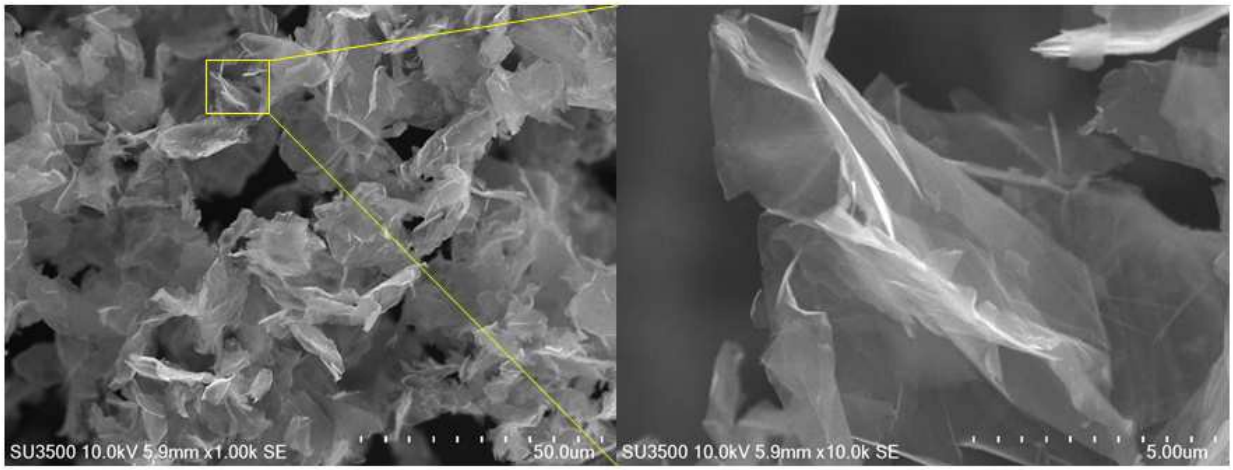

Figure 1. The SEM images of the MLG. The MLG reveals a size of several tens of microns and stacked from several graphene sheets.

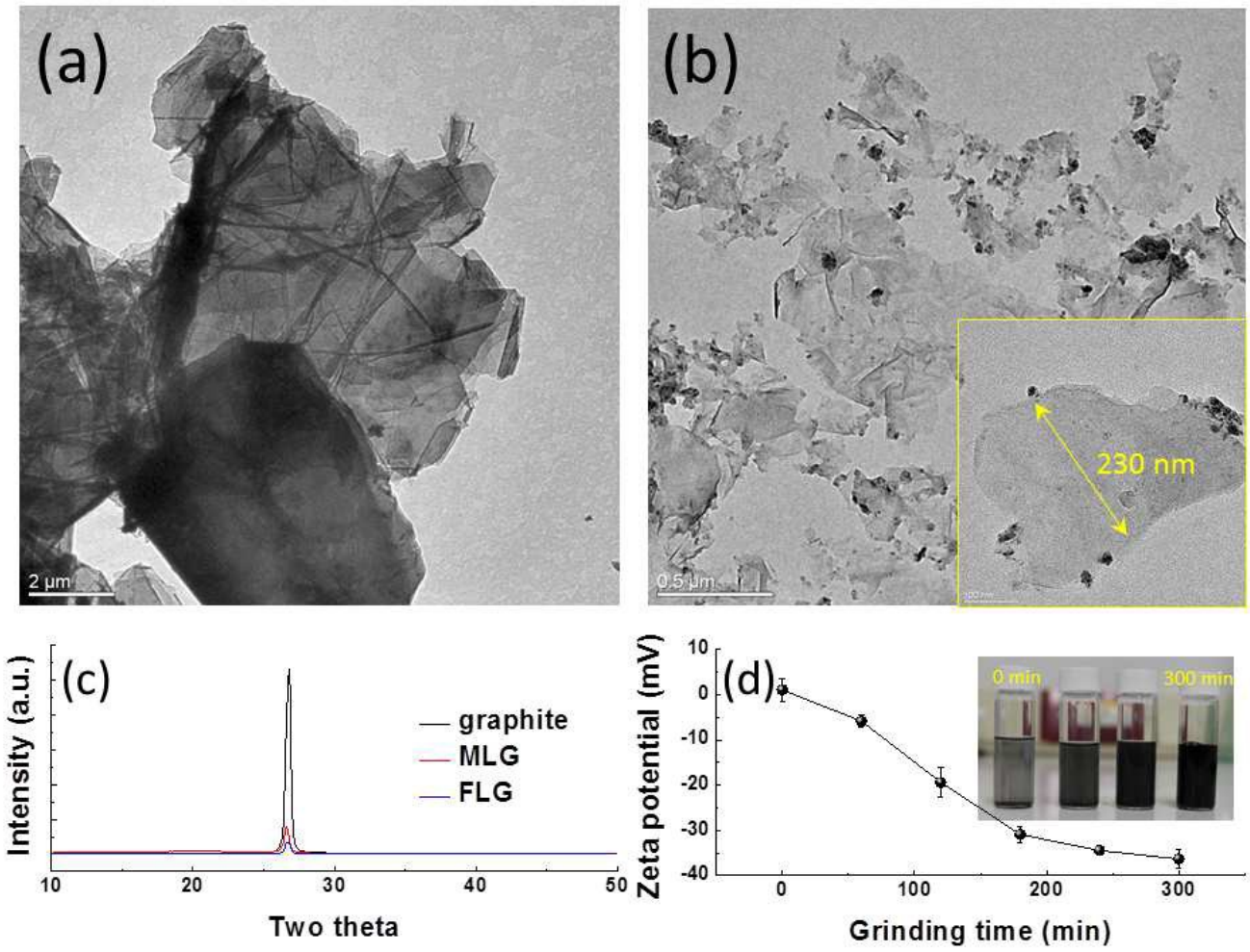

Figure 2. FLG prepared from grinding process. (a) TEM image of the MLG sample without grinding treatment; (b) TEM image of the FLG with grinding for 300 min; (c) XRD patterns of the graphite, MLG and FLG; (d) Zeta-potential measurment of FLG with differnet grinding times. (Inset: Images of the FLG solutions after various grinding times). The MLG can experience further exfoliation during brinding treatment, resulting in stable colloidal dispersion over 3 months without precipitation.

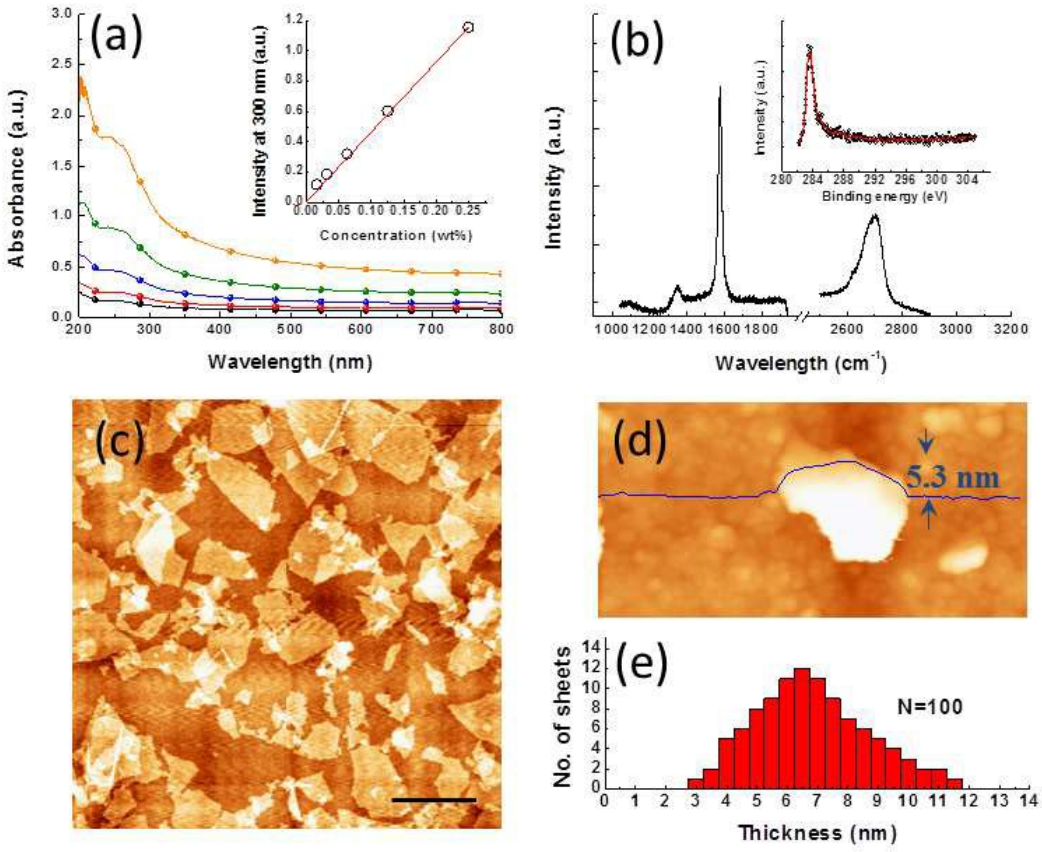

Figure 3. Characterization of the as-prepared FLG. (a) UV-vis spectra of FLG dispersion at different concentrations. Inset is a plot of absorption intensity versus FLG concentration; (b) Raman spectra of MLG and FLG. Inset is XPS spectrum of FLG; (c) a typical AFM image of FLGs on SiO_2 substrate. Scale bar: 5 μm; (d) AFM image of a single FLG with smooth planar structure. Scale bar: 250 nm; (e) thickness distribution of 100 FLG sheets. The thickness and sheet size of MLG can be reduced significantly during the grinding process leading to well-dispersed FLG solution.

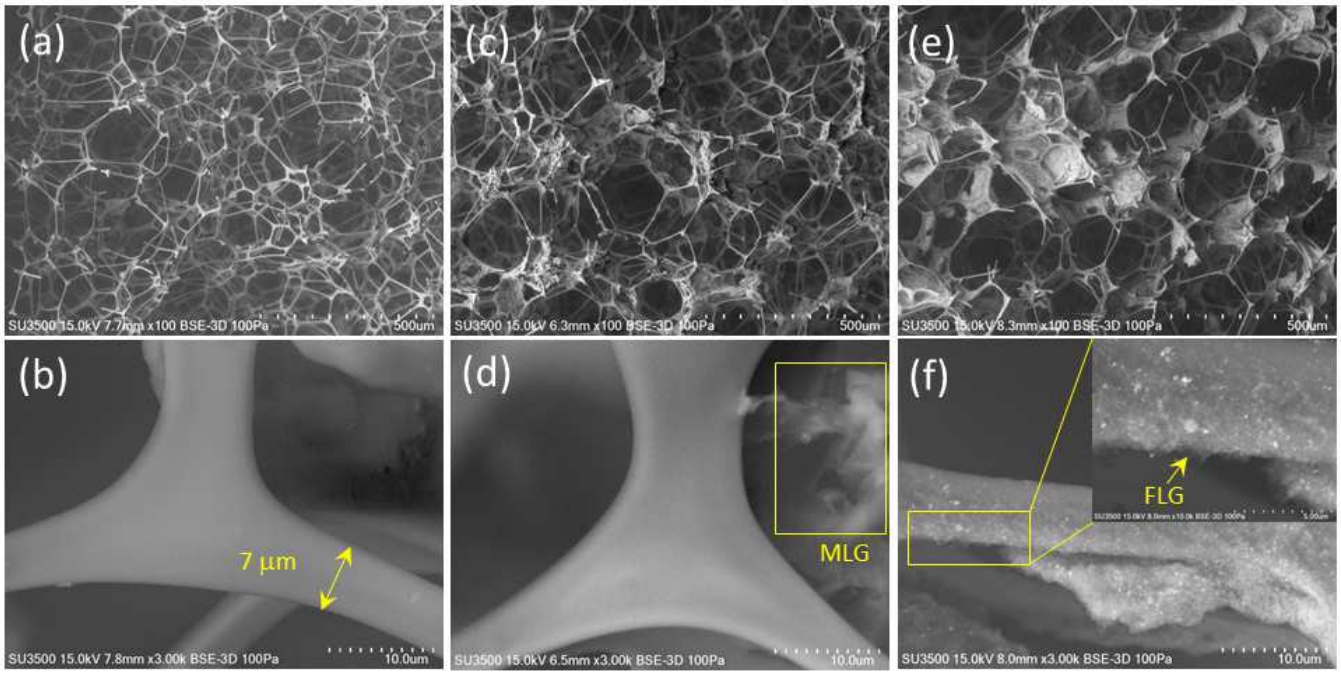

Figure 4. The typical SEM images of the pure and modified sponges with different magnification. (a, b) pure sponge; (c, d) MLG-sponge and (e, f) FLG-sponge. Inset is the higher magnification SEM image. It can be seen that the FLG reveal a better mechanical flexibility due to its favorable morphology. Therefore, it can be easily deposited on the surface of the sponge through the strong van der Waals interactions between the sponge and FLG.

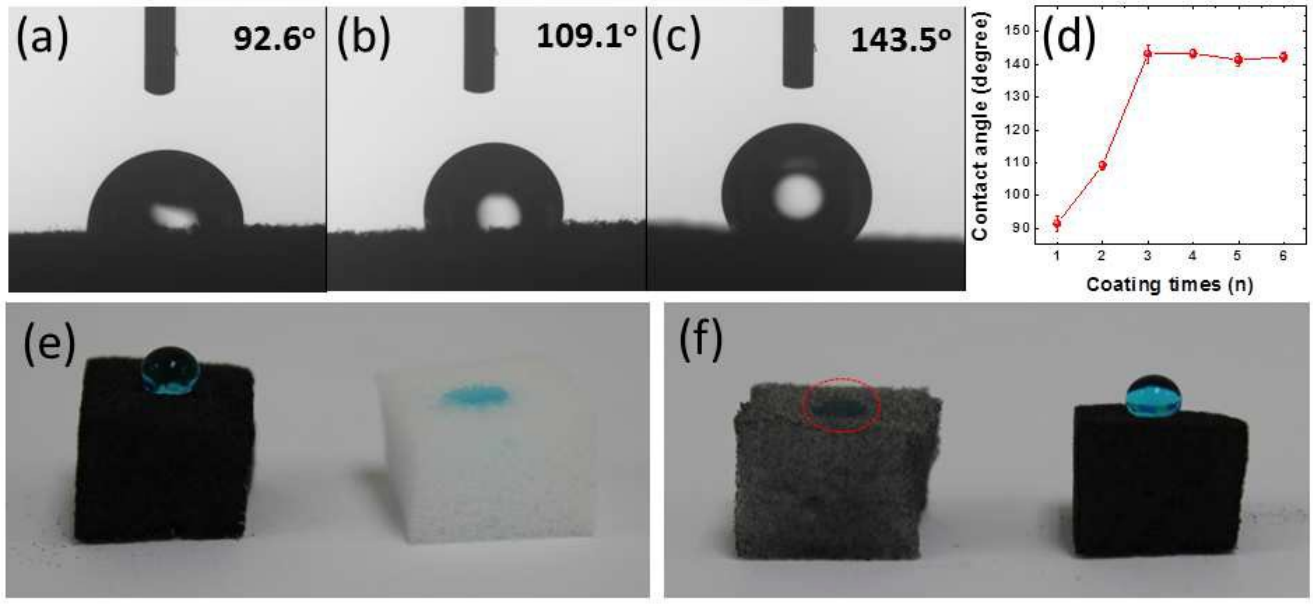

Figure 5. Superhydrophobic property of FLG-sponge. Optical image of water droplet on FLG-sponge with different coating time. (a) one time; (b) two times; (c) three times; (d) relationship between coating time and contact angle of the FLG-sponge; (e) photograph of a water droplet on the surface of (e) FLG-sponge (black color) and pure sponge (white color); (f) MLG-sponge (gray color) and FLG-sponge. The water has been dyed with methylene blue. It can be seen that the water droplet can be supported and maintain a quasi-sphere shape on the surface of FLG-sponge, indicating its superhydrophobic property. However, the water droplets were immediately absorbed by the pure sponge and MLG-sponge.

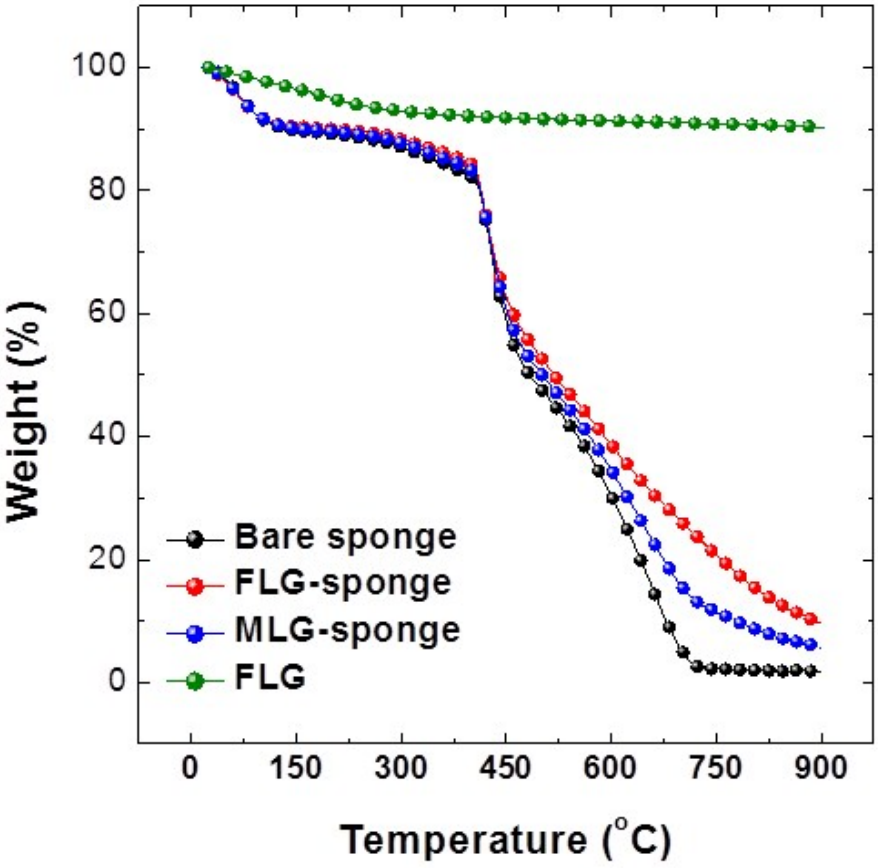

Figure 6. The TGA curves of bare sponge, FLG-sponge, MLG-sponge and FLG powder. The residual weight of FLG-sponge is larger than that of MLG-sponge after heating at 900 ^{o}C, suggesting that the physically adhesive amount of graphene is larger. This is contributed form the better mechanical flexibility and smaller size of FLG compared with that of MLG.

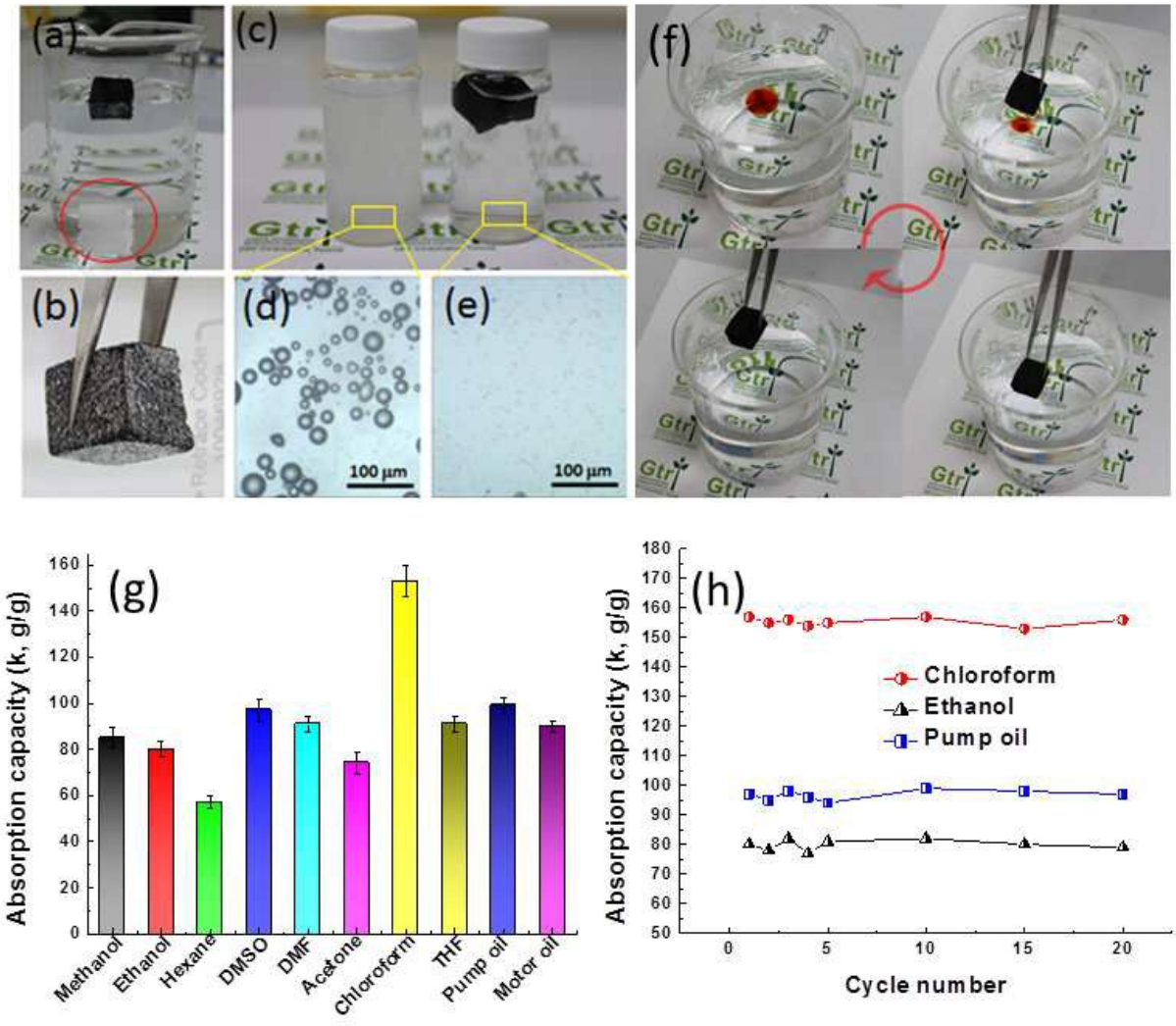

Figure 7. The oil asorption performance of FLG-sponge. (a) photograph of bare sponge and FLG-sponge after being placed on water; (b) mirror-reflection can be observed when the FLG-spongewas immersed into water, which is a convictive and direct evidence for proving the hydrophobicity of FLG-sponge; (c) photographs of the water/toluene emulsion before and after separation; (d) the optical microscope images of the water/toluene emulsion before and (e) after separation; (f) snapshots of the removal process of motor oil by using FLG-sponge; (g) absorption capacity of the FLG-sponge on various organic liquids and oils. *k* here is defined as $k=(W_{saturated\ absorption}-W_{initial})/W_{initial}$. (h) absorption recyclability of the FLG-sponge for chloroform, ethanol and pump oil.